Effective Properties of Particle Reinforced Polymeric Mould Material Towards Reducing Cooling Time in Soft Tooling Process

A. K. Nandi,[1] S. Datta,[2] J. Orkus[3]

[1]*Central Mechanical Engineering Research Institute(CSIR), MG Avenue, Durgapur-713209, West Bengal, India*
[2]*School of Materials Science and Engineering, Bengal Engineering and Science University, Shibpur, Howrah 711103, India*
[3]*Aalto University, School of Engineering, Department of Engineering Design and Production, Foundry Engineering, P.O. Box 14300, FI-00076 Aalto, Finland*

Received 10 February 2011; accepted 7 April 2011
DOI 10.1002/app.34654
Published online 2 November 2011 in Wiley Online Library (wileyonlinelibrary.com).

ABSTRACT: Cooling time in soft tooling process using conventional mold materials is normally high. Although increase of effective thermal conductivity of mold material by inclusion of high thermally conductive fillers reduces the cooling time, it affects other properties (namely, stiffness of mold box and flow ability of melt mold material), which play important roles in soft tooling process. Therefore, to apply composite polymer in soft tooling process as mold material simultaneous studies of these properties are important. In this work, extensive experimental studies are made on the effective thermal conductivity, modulus of elasticity and viscosity of composite polymeric mold materials namely Polyurethane and RTV (Room Temperature Vulcanizing)-2 silicone rubber, with aluminum and graphite particle reinforcements. To find suitable models of the effective properties of composite mold materials, which are required to decide the optimum amount of filler content before actual application, attempts are made to fit the experimental results using various models reported in the literature. Finally, different aspects in reducing cooling time in soft tooling process and further activities are reported. © 2011 Wiley Periodicals, Inc. J Appl Polym Sci 124: 2567–2581, 2012

Key words: polymer composite; particle-reinforcement; effective properties; cooling time in soft tooling

INTRODUCTION

Several reactive polymeric materials (also called flexible mold materials) are used for making mold in soft tooling (ST) process. ST process is particularly suitable for producing wax/plastic patterns (that are used in investment casting process) in small batches by vacuum assisted or gravity casting method based on RP (rapid prototype)/other patterns.[1] A method of developing metal components through rapid prototyping (RP)-soft tooling-investment casting process is illustrated in Figure 1. Because of low thermal conductivity of flexible mold materials, the wax/plastic patterns takes longer time for solidification because of their poor heat flow rate through the mold wall. To increase the heat flow rate, enhancement of thermal conductivity of mold material is essential, which can be achieved either by molecular orientation of polymer to synthesize new (highly conductive) polymeric material or by the addition of conductive fillers into the mold material. Addition of conductive fillers (particularly in the form of particles) into the mold material is a simple method that may be easily implemented in practical applications.

Significant amount of research work were found where particulate filler materials were introduced in polymer to increase its effective thermal conductivity.[2–24] The equivalent thermal conductivity (ETC) of particulate filled polymer composites was also investigated with the variation of various morphological properties of conductive filler particles,[25] multimodal particle size mixing[26] as well as using hybrid filler materials.[27] Moreover addition of filler particles in mold material as in one hand, is improving thermal properties, on the other hand, simultaneously increasing the strength and rigidity (mechanical properties)[28,29] and reducing the flow-ability of the mold material in molten condition by raising its effective viscosity.[30,31] Higher value of elastic modulus is not desirable in soft tooling as it increases mold's stiffness and affects other mold characteristics. Therefore, simultaneous studies of the influences of filler particles on equivalent thermal, mechanical, and viscous properties of particle reinforced flexible mold materials are important.

Correspondence to: A. K. Nandi (nandiarup@yahoo.com or nandi@cmeri.res.in).

Contract grant sponsor: DIT (Department of Information Technology), New Delhi, India; contract grant number: Ref No. 31(1)/2007-IEAD.

Contract grant sponsor: DST (Department of Science and Technology), New Delhi, India; contract grant number: Ref. No. SR/BY/E-09/07.

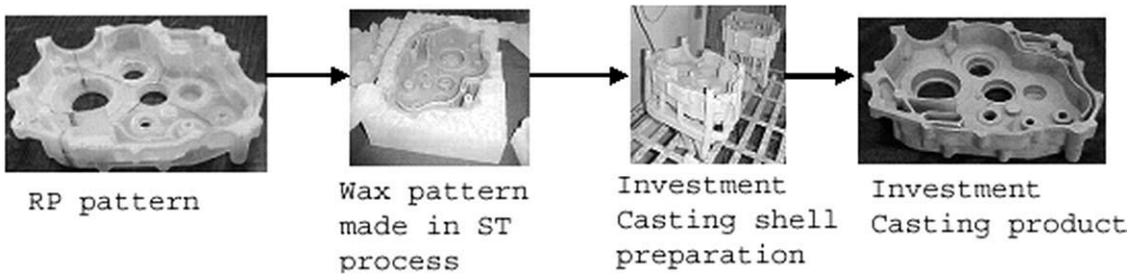

Figure 1 Development of metal components through RP -ST -Wax pattern -Investment Casting.

In this study, we have considered two different flexible mold materials namely, polyurethane (PU) and silicone rubber (SR), which are extensively used in soft tooling process for producing wax/plastic components. Aluminum and graphite particles are used as conductive fillers for the present investigation, as these filler materials are easily obtainable in the market in particulate form, and also are economical in industrial applications compared to other conductive filler materials. Analysis of equivalent thermal properties, mainly thermal conductivity, thermal diffusivity and heat capacity of particle-reinforced flexible mold materials are carried out, and the measurements of thermal properties are done based on transient plane heat source technique. Investigations on equivalent mechanical properties, namely modulus of elasticity of composite flexible mold materials, are performed using tensile testing machine. The flow-ability of melt suspensions (reinforced flexible mold materials) is examined by analyzing its equivalent viscosity/relative viscosity using rotational rheometer.

To apply composite mold material in real applications, it is important to decide the optimum amount of filler content, which needs suitable models. In this study a comparative study is carried out to fit the obtained experimental results using various models reported in the literature, to find suitable models describing the effective properties of composite mold materials. Finally, the effect on cooling time is experimentally verified with Al particle reinforced PU mold material in considering a case of manufacturing of a typical wax pattern in soft tooling process.

MATERIALS AND COMPOSITE MANUFACTURING

Among various mold materials, in this study two flexible mold materials are chosen, which are extensively used in industries, namely polyurethane (PU) produced by Smooth-ON, Inc. USA and silicone rubber (SR) (Silicones ELASTOSIL® RT 601 A) manufactured by Wacker-Chemie GMBH, Germany. Both PU and SR are of two parts (part A and part B) mixing in the ratio of 1 : 1 and 9 : 1 either in weight or volume, respectively, and cured at room temperature. The value of density of the mixed PU is 1.04 g/cm^3 and that of mixed SR is1.02 g/cm^3. The experimentally measured values of modulus of elasticity of cured PU and SR are 1631.2 N/mm^2 and 723.6 N/mm^2, respectively. The Poisson's ratio of PU possesses the value of 0.496 and that of SR is 0.499. Considering the cured PU and SR behave quasi-isotropic and quasi-homogeneous, calculated values of shear and bulk modulus of PU are found as 545.187 N/mm^2 and 67,966.667 N/mm^2, respectively, and those of SR are 241.361 N/mm^2 and 12,0600 N/mm^2, respectively.

The filler materials considered in this work are aluminum (Al) fine powder and simple (uncoated) bulk synthetic graphite (Gr) fine powder, having thermal conductivities 237 W/mK and 209.34 W/mK respectively. Both the fillers are produced by M/s LOBA Chemie Pvt. Ltd., India. The value of modulus of elasticity of Al is considered as 70,000

TABLE I
Information About the Prepared Compounds with Varying Filler Contents

Composite	Matrix material	Graphite powder (Vol%)	Aluminum powder (vol %)
1	Polyurethane	3.1	6.6
2		10.0	9.3
3		15.1	13.1
4		22.1	16.6
5		24.4	19.9
6		29.6	23.1
7		35.0	34.9
8		39.6	39.9
9		–	44.9
10		–	48.6
11	Silicone rubber	5.0	5.0
12		12.8	10.0
13		14.4	15.1
14		20.0	19.9
15		25.2	24.9
16		30.8	30.0
17		34.8	40.0
18		40.2	45.8
19		–	47.5
20		–	50.0

TABLE II
Filler Particle Size and Shape Distributions

Filler type	Size distributions				Shape distributions		
Gr	From 0.1 mm to 0.3 mm	Above 0.3 mm to 0.5 mm	Above 0.5 mm to 1.0 mm	Above 1.0 mm	Spherical	Cylindrical	Irregular
	72%	18%	8%	2%	30%	27%	43%
Al	From 1 μm to 10 μm	Above 10 μm to 30 μm	Above 30 μm to 50 μm	Above 50 μm	Spherical	Cylindrical	Irregular
	66%	24%	8%	2%	46%	22%	32%

N/mm^2 and that of synthetic graphite fillers is taken as 25,500 N/mm^2. The values of shear and bulk modulus of aluminum are 26,000 N/mm^2 and 76,000 N/mm^2 respectively, and those of graphite (poisons ratio = 0.31) are 9700 N/mm^2 and 22,902.7 N/mm^2, respectively. Table I describes information about the prepared compounds with varying filler contents.

Measurements of granulometric parameters for both the fillers are made using M420, WILD Heerbrugg Microscope. The particle size and shape distributions of both filler materials are listed in Table II. To understand the particle size and shape distributions, the morphologies of particles of both the filler materials are illustrated in Figure 2 by showing enlarge images (taken using Nikon EPIPHOT 200 microscope) of some sample particles taken at random. The (arithmetic mean) size of particles is determined by taking the average of minimum and maximum lengths of the sample particles. For near spherical shape, the particle size is equivalent to the diameter of sphere. For near cylindrical shape, the size of particle is equal to (length + diameter)/2. To find the size distribution of particles, a small amount of sample is taken at random from the bulk. Then the number of particles is counted as well as the size of each particle is measured in an approximate approach and finally determined the particle size distributions arithmetically in four different ranges. The average particle sizes (calculated based on weighted average method) of aluminum and graphite fillers are found as 12.3 μm and 296 μm, respectively. The maximum packing fractions of graphite and aluminum particles found experimentally are 0.5216 and 0.6032, respectively. The (maximum) packing fraction of (particulate) filler is defined by the ratio of apparent density (ρ_{app}) to actual density (ρ_a) of filler material. To determine the apparent density of filler, a certain amount of filler (which is dried in vacuum) is weighted accurately. After that, the dried filler particles are poured into a vessel (which is a laboratory test tube with different marking on its surface indicating the volume label) and then, the vessel is shaken sufficiently with the help of laboratory shaking machine until volume of filler in the vessel becomes constant or the volume of test tube occupied by the filler becomes minimum. In this condition, the apparent volume of the filler is measured from the marking on the test tube surface and the apparent density is calculated by dividing the weight of the filler by its apparent volume. We have carried out the test five times for each of the fillers with different amount of fillers ranging from 10 to 20 cc. The above-mentioned value of maximum packing fraction is the average of 5 test results with standard deviations 0.0146 and 0.0168 for the graphite and aluminum particles, respectively.

Before preparing the composite samples for various tests, the weights of part-A and part-B of polymer (PU/SR) and filler are calculated based on the respective densities of these components for a certain volume fraction of filler in the composite. Then,

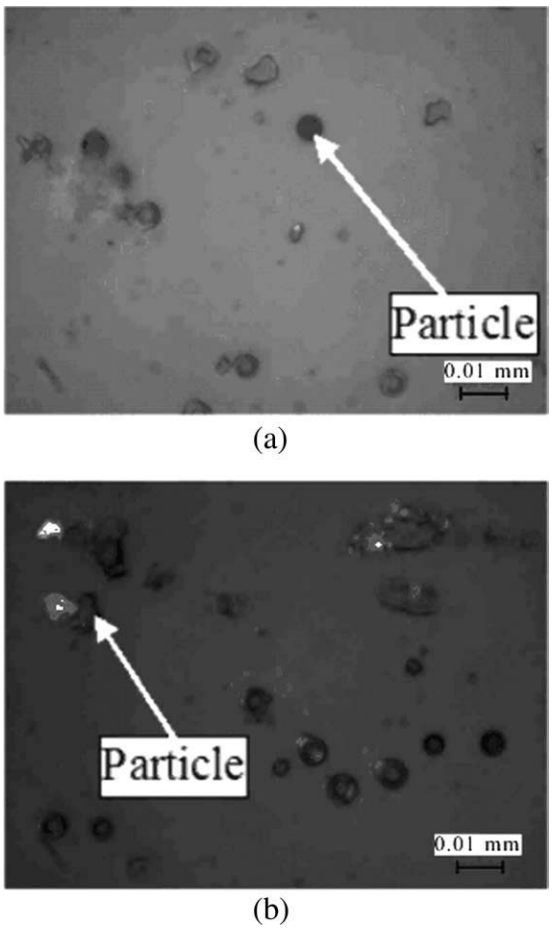

Figure 2 Morphology of filler particles (a) Al fine powder (b) Graphite particles.

the part A (liquid polymer) is first mixed with filler particles in a container using manual stirring. To assure a uniform mixing, stirring of liquid polymer and gradual pouring of filler material is done simultaneously. Once, the uniform mixing of liquid polymer and filler material is achieved, the hardener (Part B) is poured into the mixture of liquid polymer and filler, and stirred it properly for another 5–10 min. Part B (hardener) for silicone rubber materials is a silane compound, which comprises of a 2-hydroxy-propionic acid alkyl ester radical. Part A of Polyurethane consists of Disononylphthalate and Toluene Diisocyanate, whereas Distillate (petroleum), hydrotreated heavy naphthenic, Diethyltoluenediamine and Phenylmercuric neodecanoate are the ingredients of Part B of PU. Curing of polymers starts after a certain time of mixing both the Part A and Part B, which is called pot life. The pot life of SR and PU used in this study are normally withstanding around 90 min and 30 min, respectively, at 23°C. Before pouring the (melt) mixture material into mold box, release agent is sprayed thoroughly on the inside surface of the mold box. Once curing of the polymer composite is done at room temperature, it is taken out from mold box by cutting along a suitable parting line. After rubber has cured at room temperature, the mold rubber is kept in the post curing temperature, 65°C in case of PU and 40° for SR for 4–8 h which will increase its physical properties and performances. Then, both the parts of mold box are assembled in the proper position with the help of adhesive tape. Once, the mold is prepared, liquid wax is poured into the mold box, and cooling/solidification of liquid wax is (normally) done in room temperature. Different samples are prepared by varying the amount of (volume fraction) filler mixed with PU and SR separately. The amount of filler to be mixed with mold material (PR/SR) is restricted up to the maximum packing fraction of filler particles, since it signifies the maximum loading level of particles to be mixed into a fluid.

EQUIVALENT THERMAL PROPERTIES

Experimental measurements: Procedures and numerical formulations

Equivalent thermal properties of different composites are measured based on transient plane heat source (TPS) hot disk method[32] following the standard, ISO 22007-2: 2008(E). The instrument, TPS 2500 S Thermal Conductivity System associated with the software, HotDisk Thermal Constant Analyzer V.5.9.5[33–35] is used. The TPS 2500 S Thermal Conductivity System utilizes a hot disk sensor in the shape of a double spiral of nickel wire. The hot disk sensor (design number: C5501) with m (=14) concentric rings is used here for measuring thermal properties. The sensor element is made of 10 μm thick nickel wire and the spiral is supported by 30 μm thick Kapton material to protect its particular shape by providing sufficient mechanical strength, and also to keep it electrically insulated. The relaxation time of the probe is less than 10 min, and duration of 15 min is allowed to reach a constant temperature difference. The sensor used in the experimentation has a diameter of 2a (where a, the radius of largest ring equals to 6.403 mm) and the total thickness (Kapton-nickel-Kapton) of 2v (=70 μm) was placed between two samples of 50 mm square and thickness of 5–6 mm. The probing depth of the sensor used for all the samples is around 6 mm. In hot disk method, measurements of thermal properties are made based on the average temperature increase, $\Delta\overline{T}(\tau)$ at time t in hot disk sensor, which is expressed at any position (designated as $\vec{r} = (r, \theta, z)$) in the sample as

$$\Delta\overline{T}(\tau) = \frac{1}{\Pi a(m+1)} \times \frac{P_0}{{}^2\Pi^{3/2} am(m+1)k} \times \int_0^\tau \frac{d\sigma}{\sigma^2} \sum_{n=1}^{m} \frac{na}{m} \sum_{l=1}^{m} l_e \frac{-\left((r/a)^2+(1/m)^2\right)}{4\sigma^2} I_0\left(\frac{n1}{2m^2\sigma^2}\right) 2\Pi = \frac{P_0}{\Pi^{3/2} ak} \times \frac{1}{m^2(m+1)^2} \times \int_0^\tau \frac{d\sigma}{\sigma^2} \sum_{n=1}^{m} n \sum_{l=1}^{m} l_e \frac{-\left((r/a)^2+(l/m)^2\right)}{4\sigma^2} I_0\left(\frac{nl}{2m^2\sigma^2}\right) = \frac{P_0}{\Pi^{3/2} ak} D(\tau), \quad (1)$$

where k is thermal conductivity of materials and P_0 is the power output of the hot disk sensor per unit time. $D(\tau)$ is a dimensionless time function. σ is an integration variable that is defined as $\sqrt{\frac{\alpha(t-t')}{a^2}}$, and the (dimensionless) parameter, $\tau(=\frac{\sqrt{\alpha t}}{a})$ is called the characteristic time ratio, where α (=k/ρc) is the thermal diffusivity, where ρ and c are the density and specific heat of the material respectively. A more detailed derivation of average temperature increase in hot disk sensor can be found in.[36]

From eq. (1), it is seen that average temperature increase in hot disk sensor, $\Delta\overline{T}(\tau)$ is linearly proportional with the dimensionless time function,$D(\tau)$ and exhibited straight-line curve by plotting there values. The slope of this straight-line curve is equal to $\frac{P_0}{\Pi^{3/2} ak}$ from which the value of k may be evaluated. But, the straight line curve between $\Delta\overline{T}(\tau)$ and $D(\tau)$ may be obtained for a proper value of τ, that depends again on the value of α (for a given value of a and time, t). Therefore, it is required to find the proper

value of α and normally this may be done by making a series of computational plots of $\Delta\overline{T}(\tau)$ versus $D(\tau)$ for a range of α value. The correct value of α will be reached once the straight-line plot of $\Delta\overline{T}(\tau)$ versus $D(\tau)$ is obtained. Once the correct value of α is obtained, the value of k can be determined from the slope of the straight-line plot of $\Delta\overline{T}(\tau)$ versus $D(\tau)$.

Another way to determine the value of k is to measure the density (ρ) and the specific heat (c) of the material separately. Then, the value of k can be obtained by multiplying the value of α with the density and specific heat of the material. This method is generally applied for anisotropic materials. If the properties along x- and y-axes are the same, but different from those along the z-axis and if the plane of the hot disk sensor is mapped out by x- and y-axes, the eq. (1) will be expressed as

$$\Delta\overline{T}(\tau_x) = \frac{P_0}{\Pi^{3/2} a\sqrt{k_x k_z}} D(\tau_x), \tag{2}$$

where k_x and k_z are the thermal conductivities in the x (or y) and z directions respectively, and $\tau_x = \frac{\sqrt{\alpha_x t}}{a}$. The value of α_x can be determined by the above stated iteration process until a straight-line plot of $\Delta\overline{T}(\tau_x)$ verses $D(\tau_x)$ is reached and the value k_x is equivalent to $\alpha\rho c$. On the other hand, from the slope of the straight-line plot of $\Delta\overline{T}(\tau_x)$ versus $D(\tau_x)$, the value of $\sqrt{k_x k_z}$ can be found out. Therefore, the value of k_z is calculated by dividing the value of $\sqrt{k_x k_z}$ by obtained value of k_x.

RESULTS AND DISCUSSION

The values of equivalent thermal conductivity (ETC), thermal diffusivity and volumetric heat capacity of particulate filled PU and SR composites with Al and graphite particles for different amount of filling fraction, as obtained through experimentations at room temperature (23°C), are illustrated in Figure 3. The test samples prepared for measuring effective properties are tried to make void free as much as possible. For this reason, special care has been taken during manufacturing of the samples. The values of the results shown in the figures for each case are the mean of measurements of more than one sample. However, the number of samples is varied from five to ten in different cases. From the experimental results [Fig. 3(a)], it is quite evident that thermal conductivities of particulate filled PU and SR are increasing (around 10 times) with increasing amount of filler and the increasing rate starts drastically more at around 20–30% volume fraction of filler for some composites. This is due to the formation of thermally conductive chain(s) in the composite whose tendency is high in elevated filler content. In Figure 3(a), another point is noticed that increasing rate of thermal conductivity is comparatively higher for any level of filler content when graphite filler is used for both the mold materials (PU and SR). The reason is that large particles, which are equivalent as the composed of aggregates of filler particles, are better capable of forming conductive chains than fine particles. Moreover, the amount of heat scattered around the contact points in case of coarse particles is smaller than fine particles, since less number of contact points required to form the same length of conductive chain.[37] Therefore, the effective thermal conductivity of a particle reinforced flexible (polymeric) composite depends on conductivity of the polymer, the thermal conductivity of the filler material, amount of filler content in the composite, and the size and shape distributions of filler particles as well.

On the other hand, it is worth mentioning that manufacturing process of composite is also an important aspect to achieve a maximum value of ETC of flexible mold material composites. Because there is much possibility of existence of voids in the mold due to fault(s) occurred during manufacturing. The presence of voids will reduce the effective thermal conductivity of the mold. To demonstrate such kind of phenomenon, two PU-Al composite samples are considered whose morphological structures are shown in Figure 4. It has been found that though the composite contains higher filler (48.66%), it exhibits lower ETC (0.94 W/mK) than the ETC (1.25 W/mK) of composite having lower (39.922%) filler content due to presence of more voids.

Equivalent thermal conductivity model

Figures 5(a,b) show the effort to describe the experimental results of ETC of the four kinds of composite using by several empirical/semiempirical models, namely the model proposed by Agari-Uno [38], Maxwell-Eucken [39], Cheng-Vackon [40], Ziebland relation discussed by Butta and Migliares in [41], Bruggeman [42], Lewis-Nielsen [43] and Torquato [44]. In the Figure 5, the experimental values of ETC of particle reinforced mold composites are shown as data points whereas the models are represented by the lines with different styles and symbols corresponding to different models. It is observed that Lewis-Nielsen model[43] [which is defined by empirical expression as shown in eq. (3)] provides closer estimations (average % error, 28.48) than other empirical models in all four composites.

$$k_c = \frac{1 + AB_{V_f}}{1 - B_{V_f}\varphi} \times k_p, \tag{3}$$

where $B = \frac{\frac{k_f}{k_p} - 1}{\frac{k_f}{k_p} + A}$ and $\varphi = 1 + \left(\frac{1-\varphi_m}{\varphi_m^2}\right) \times V_f$

k_c, k_p, and k_f represent the equivalent thermal conductivities of composite, polymer, and filler, respectively, and V_f is the volumetric fraction of filler in

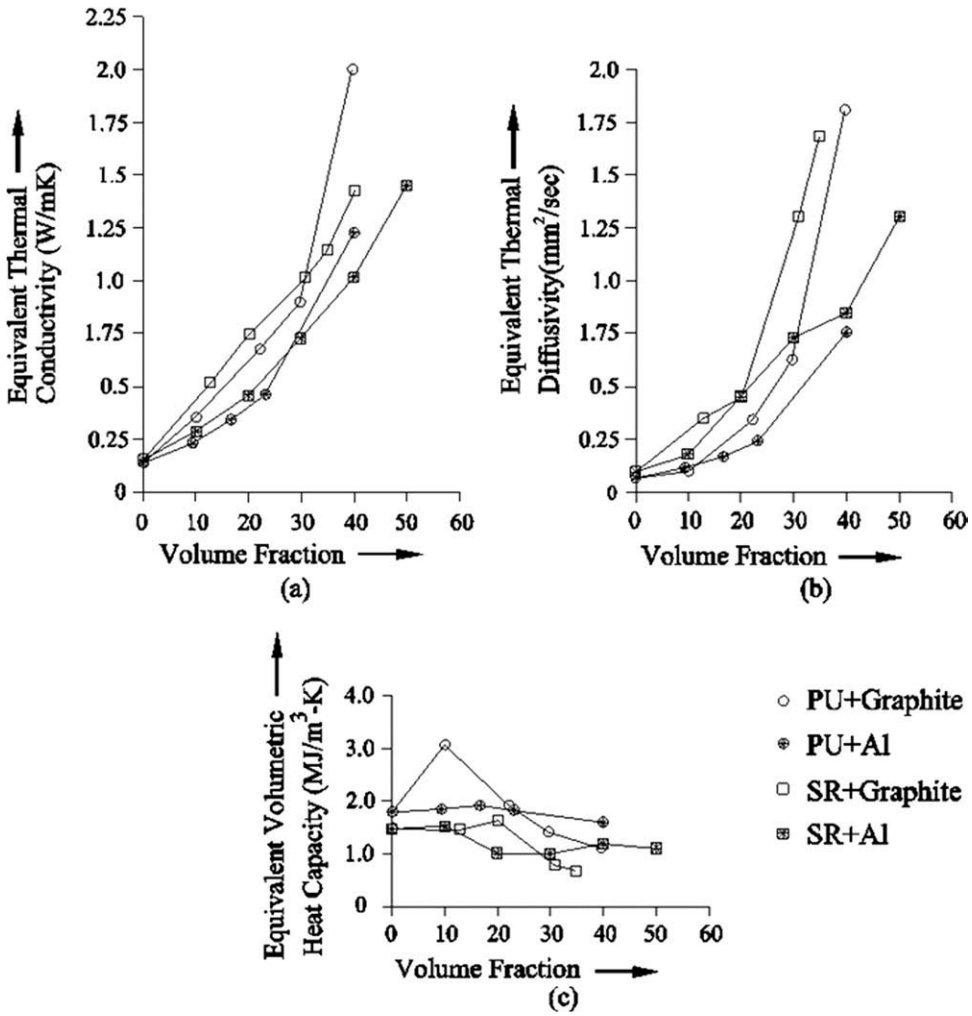

Figure 3 Equivalent thermal properties of PU and SR composites with aluminum and graphite particles: (a) thermal conductivity (b) thermal diffusivity (c) volumetric heat capacity.

the composite. The constant A depends on the shape and orientation of dispersed particles in the composite, and is defined by $A = k_E - 1$ (where k_E is the Einstein coefficient). φ_m is the maximum packing fraction of disperse phase (for randomly distributed spherical particles, $\varphi_m = 0.637$). The value of A is equal to 1.5 for randomly distributed spherical particles, while in case of randomly distributed aggregates of spherical particles, $A = 3$.

Moreover, a better fit is observed with the semi-empirical model of Agari-Uno[38] [expressed by eq. (4)] whose controlling parameters are determined

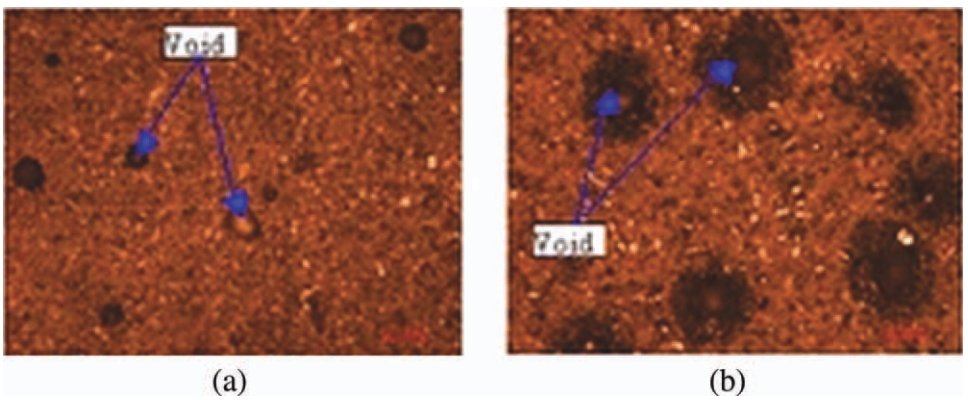

Figure 4 Morphological structure of PU and aluminum composites with volume fraction levels: (a) 39.922% (b) 48.664%. [Color figure can be viewed in the online issue, which is available at wileyonlinelibrary.com.]

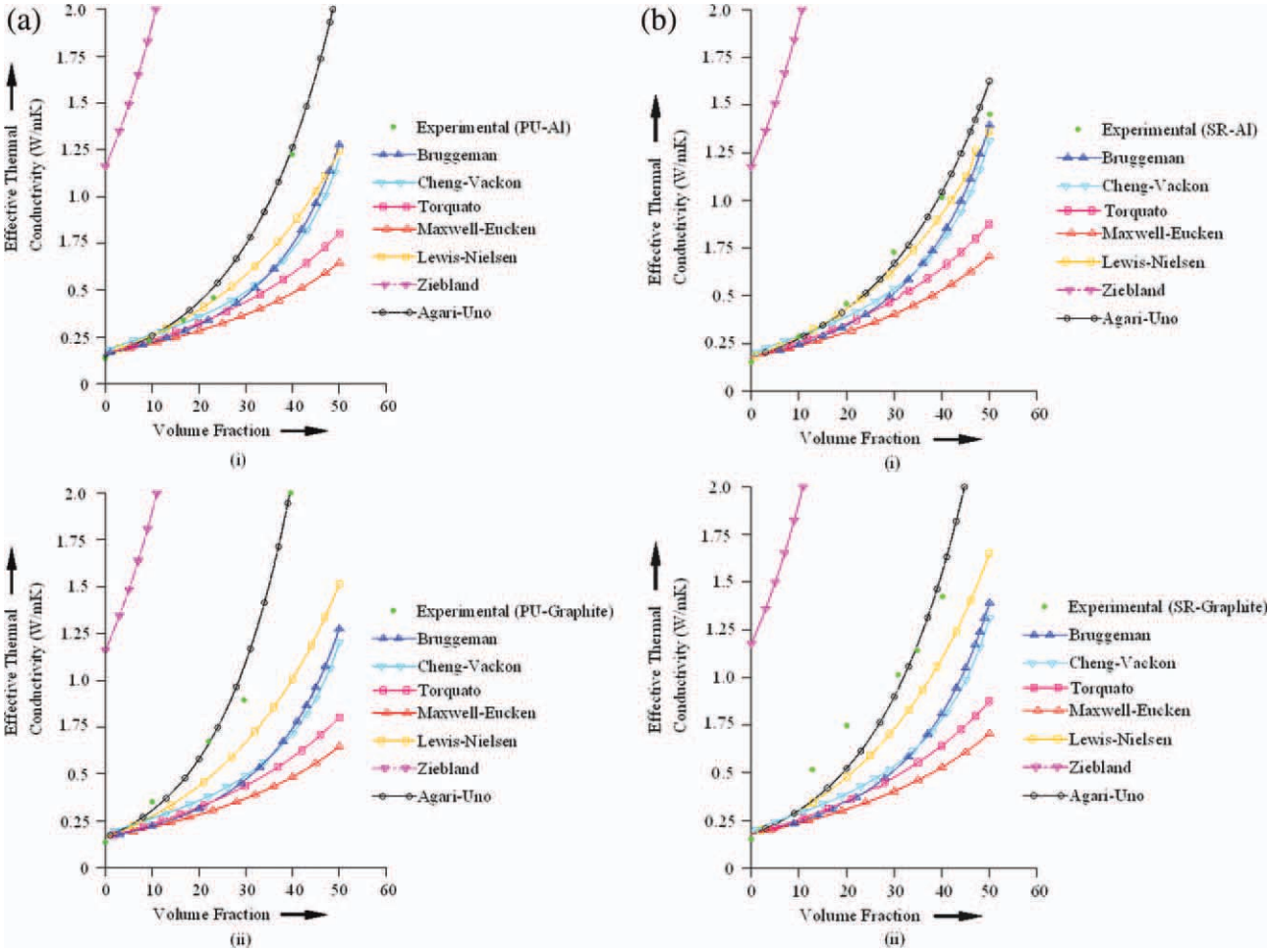

Figure 5 (a) Thermal conductivities of composites (i) PU-Al (ii) PU-Graphite: experimental values and various model predictions. (b) Thermal conductivities of composites (i) SR-Al (ii) SR-Graphite: experimental values and various model predictions. [Color figure can be viewed in the online issue, which is available at wileyonlinelibrary.com.]

based on the experimental data. The average % errors of Agari-Uno model are found as 2.35, 10.12, 8.9, and 16.82 by individually fitting the composite systems mentioned in Figures 5(a,b), respectively. However, it was found that the average % error of Agari-Uno model by fitting all the data of four composite systems is considerably high, (19.29%) though still lower than Lewis-Nielsen model.

$$\ln k_c = V_f C_2 \ln k_f + (1 - V_f)\ln(C_1 k_p), \qquad (4)$$

where C_1, the factor of the effect on crystallinity and crystal size of polymer, does not depend on particle size. C_2 is the factor of ease in forming conductive chains of particles, which is affected by filler particle size.

In looking at the Agari-Uno models, it was found that values of C_1 (0.933594, 1.0, 1.0, and 1.0) are nearer/equal to 1.0 and the values C_2 are 0.625, 0.852295, 0.4944, and 0.690013 for the suspension systems, Figures 5(a,b), respectively. Value of C_1 close to 1.0 indicates that effect of crystallinity and crystal size of polymer on the changing thermal conductivity of polymer (matrix material) is negligible due to the inclusion of filler. Such kind of effect is observed in flexible mold material composites with both the graphite and Al particles. The value of C_2 close to 1.0 indicates more ease in forming conductive chains of filler particles in composite. In the present composites, it is observed that the value of C_2 is greater for large particle size filler (graphite) than the smaller one (Al), which agrees well with the results of Boudenne et al.[3]

EQUIVALENT MODULUS OF ELASTICITY

Experimental measurements: procedures

Modulus of elasticity of a material may be tested using different standard test methods, namely tensile testing, four-point loading test,[45] ultrasonic measurement,[46] etc. Here the tensile testing method is adopted to find the equivalent Young's modulus of flexible mold material composites. The experimen-

tations are carried out based on the standard, ASTM D 3039*M*-08. According to this standard, a constant rectangular cross section shaped specimen of thickness, 2.5 mm ± 4%, 25 mm ± 1% of width and 270 mm of length in the form of sheet is prepared. Tensile tests are performed on an Instron testing machine (made of DARTEC). An extensometer (Made of MTS, Model No. 634.25F-24, Serial No. 10288577A) is used to measure the strain. The values of displacement, force and strain are recorded through data acquisition system at a constant interval of 0.01 s. After plotting the data of stress versus strain, a linear curve is found which indicates the elastic region of the stress–strain diagram of the material. The slope of this linear curve is evaluated, which represents the tensile modulus of elasticity of composite mold.

Results and discussion

To find the equivalent modulus of elasticity of different particle reinforced polymeric mold material composites (SR and PU), we have considered six test samples for each case and the average of the results obtained in the six test cases is shown in the Figure 6. From the experimental results (as illustrated in Fig. 6), the increase of modulus of elasticity is observed in all kinds of flexible composite mold reinforced with conductive filler particles. However, it is noticed that the degree of enhancement of modulus of elasticity differs in different composite systems. Furthermore, increasing the rate of modulus of elasticity of each composite system is not uniform with increasing the loading of filler particles, particularly in PU composite systems.

In PU composite system, increase of modulus of elasticity is more-or-less similar in nature with both the reinforcements (Al and Graphite) especially when the filler concentration label is below 40%. But, a sudden rise of modulus of elasticity is observed in PU composite filled with Al filler at above 40% volume fraction unlike to that filled with graphite particles. This may be due to the fact that Al particles are securely embedded with polymer matrix since the size of particles is comparatively smaller than graphite particles. This phenomenon is specifically observed when the filler content is more than 40%. Whereas adhesion between PU and graphite particles is not so critical compared with polymer matrix and metallic filler composite systems. On the other hand, a comparatively uniform increasing rate is observed in SR composites filled with both types of filler (Al and graphite).

Composites of PU and SR reinforced with Al particles possess quite similar behavior in increasing modulus of elasticity at the volume fraction ranging from 10 to 40%. For any reinforcement condition, SR composite filled with Al particles deserves lower values of modulus of elasticity over the PU composite filled with Al, because cured SR possesses lower modulus of elasticity than that of PU. On the other hand, reinforcement of graphite particles does not show much difference in modulus of elasticity for both kinds of flexible mold materials. Thus, the effective modulus of elasticity of particle-filled flexible (polymeric) mold material composite also depends on the modulus of elasticity of polymer, modulus of elasticity of filler material, and the volume/weight fraction of filler particle in the composite.

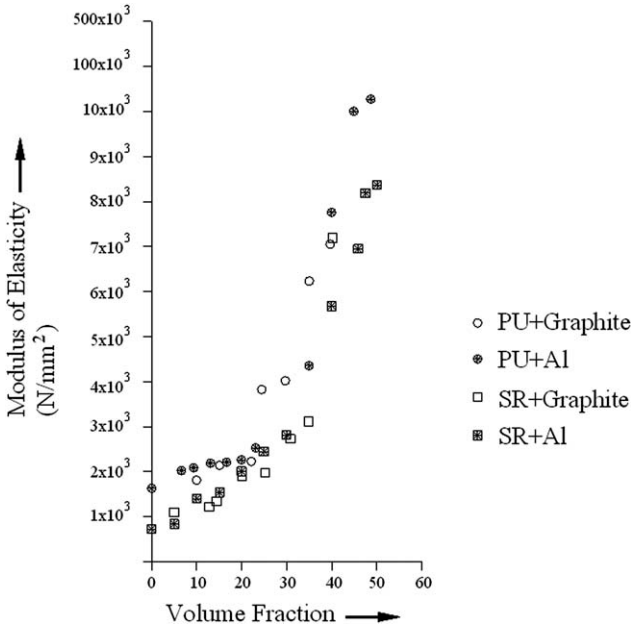

Figure 6 Equivalent modulus of elasticity of PU and SR composites with aluminum and graphite particles.

Equivalent modulus of elasticity model

The experimental results of equivalent modulus of elasticity of particulate filled polyurethane and silicone rubber composites (as illustrated in Fig. 6) are tried to explain using various existing empirical models cited in the literature. The most commonly used models for predicting equivalent modulus of elasticity of a composite material in a straightforward way from its numerical expressions are the followings.

Model proposed by Paul[47]:

$$E_C = \frac{E_m^2 + \left(E_m E_f - E_m^2\right) V_f^{2/3}}{E_m + (E_f - E_m) V_f^{2/3}\left(1 - V_f^{1/3}\right)}, \qquad (5)$$

where E_m, E_f, and E_c are the modulus of elasticity of the matrix, particle and composite material, respectively, and V_f is volume fraction of filler material.

Model proposed by Ravichandran[48]:

$$E_C^1 = \frac{\left(C_{E_m E_f + E_m^2}\right)(1+C)^2 - E_m^2 + E_f E_m}{\left(C_{E_f + E_m}\right)(1+C)^2}, \quad (6)$$

$$E_C^u = \frac{\left\lfloor E_f E_m + E_m^2(1+C)^2 - E_m^2 \right\rfloor (1+C)}{(E_f - E_m)C + E_m(1+C)^3}, \quad (7)$$

where $C = \left[\frac{1}{V_f}\right]^{1/3} - 1$

Model proposed by Wu[49]:

$$\frac{1}{E_C} = \left[\frac{1}{E_m} - \frac{\left(\frac{1}{E_m} - \frac{1}{E_f}\right)^2}{\lambda\left(\frac{1}{E_m} + \frac{V_m}{V_f E_m}\right)}\right] V_m + \frac{V_f}{E_f}, \quad (8)$$

where V_m ($=1-V_f$) is volume fraction of matrix material and λ is the parameter, which remains fixed for any relative concentration of a given composite material. Through experimental study, it has been found that the value of λ quite closes to unity for $\frac{E_m}{E_f} \ll 1$.

Besides the above models, there are many empirical expressions proposed by various researchers namely Hashin-Shtrikman bounds,[50] Halpin-Tsai models,[51,52] Walpole bounds,[53,54] methods based on mean-field (such as Voigt model,[55] Reuss model,[56] Mori-Tanaka's models,[57] etc.), self-consistent method based models,[58] models based on differential method,[59] Lielens models[60]) from which the equivalent modulus of elasticity [or its upper bound (UB) and lower bound (LB)] of a particulate filled composite can be determined based on the conventional expression [eq. (9)] of isotropic material property by assuming the composite to be (quasi) isotropic and (quasi) homogeneous.

$$E = \frac{9KG}{3K + G}, \quad (9)$$

where E, G, and K are the modulus of elasticity, shear modulus and bulk modulus of composite material, respectively.

If the Lielens model is formulated based on a normalization of the upper and lower bounds suggested by Hashim-Shtrikman, it can be written as

$$K_C = \frac{1}{\frac{1-f}{K_{H-S}^L} + \frac{f}{K_{H-S}^U}}, \quad (10)$$

$$G_C = \frac{1}{\frac{1-f}{G_{H-S}^L} + \frac{f}{G_{H-S}^U}}, \quad (11)$$

where $f = \frac{V_f + V_f^2}{2}$, and K_{H-S}^L, K_{H-S}^U, G_{H-S}^L and G_{H-S}^U are the Hashin-Shtrikman lower and upper bounds of bulk modulus and shear modulus, respectively, which are expressed by the following empirical expressions.

$$K_{H-S}^L = K_m + \frac{V_f}{\frac{1}{K_f - K_m} + \frac{3V_m}{3K_m + 4G_m}}, \quad (12)$$

$$K_{H-S}^U = K_f + \frac{V_m}{\frac{1}{K_m - K_f} + \frac{3V_f}{3K_f + 4G_m}}, \quad (13)$$

$$G_{H-S}^L = G_m + \frac{V_f}{\frac{1}{G_f - G_m} + \frac{6(K_m + 2G_m)V_m}{5G_m(3K_m + 4G_m)}}, \quad (14)$$

$$G_{H-S}^U = G_f + \frac{V_m}{\frac{1}{G_m - G_f} + \frac{6(K_f + 2G_f)V_f}{5G_f(3K_f + 4G_f)}}. \quad (15)$$

In Figure 7(a,b), the equivalent modulus of elasticity of four kinds of particle reinforced polymer composite obtained using various models are illustrated. In the Figure 7(a,b), the models are identified by the line style with a symbol positioned on the line. On the other hand the experimental values of equivalent modulus of elasticity are identified as stars (data points). Through rigorous comparative study among the experimental results with that obtained from various models, it is found that model proposed by Lielens, provides close agreement with experimental data compared to other models, particularly up to a volume fraction of 0.4 of the particulates. The reason is that the Lielens's model is formulated based on the normalization of the upper and lower bounds suggested by Hashim-Srikman [defined in eqs. (10) and (11)]. Moreover, from the Figure 7(a,b), it has been observed that most of the experimental data of all the four suspension systems lie in the region enclosed by the Hashim-Strikman upper and lower bounds. The model seems to be efficient enough to predict the modulus of elasticity of the PMCs with varying matrix as well as reinforcement particles. On the other hand, there are some models showed close agreements with the experimental results with only low particle reinforcements, such as models proposed by Wu, Kerner and Paul, as well as model developed based on differential method.

EQUIVALENT VISCOSITY OF MELTS PARTICLE REINFORCED FLEXIBLE MOLD MATERIALS

Viscosity measurements and preparation of samples

The polymer processes of flexible mold materials are shear-dominated in majority; therefore the viscosities of particulate-filled flexible mold materials are measured using shear deformation measuring devices. The viscosity of polymer (as a non-Newtonian

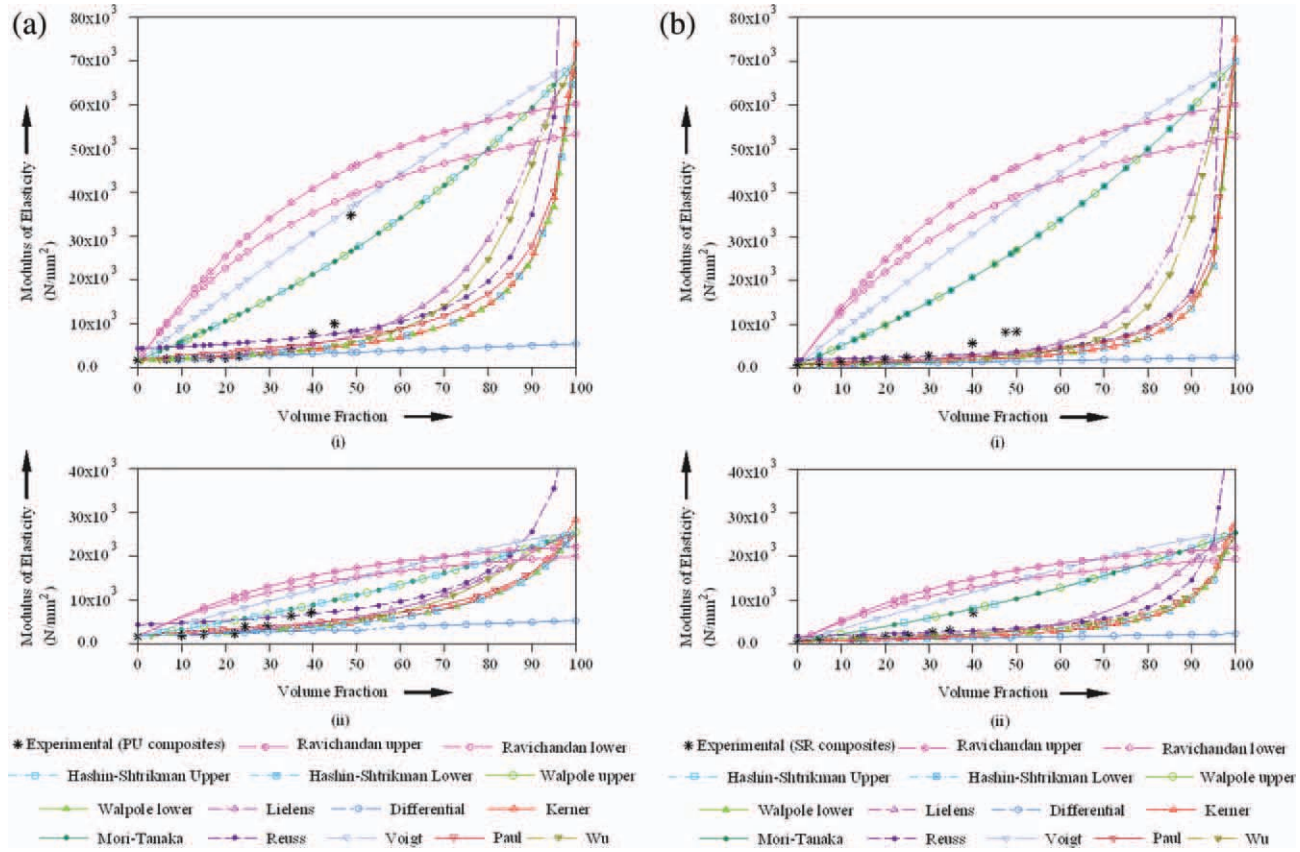

Figure 7 (a) Equivalent modulus of elasticity of composites (i) PU-Al (ii) PU-Graphite: experimental values and various models. (b) Equivalent modulus of elasticity of composites (i) SR-Al (ii) SR-Graphite: experimental values and various models. [Color figure can be viewed in the online issue, which is available at wileyonlinelibrary.com.]

viscosity) depends on both, the rate of deformation and temperature. In most soft tooling processes, the mold materials are poured into the mold box generally at room temperature and the occurrence of deformation is not significant (i.e., only the strain rate generated during normal flow of polymer melt). Therefore, it was concentrated only to the equivalent viscosity of the particulate-filled polymer at room temperature at zero strain rates. Practically, the viscosity of mold material should be low enough so that it can fill up the entire mold box in a short time. As viscosity of polymer melt decreases with increase of temperature and strain rate, it will be an added advantage for the soft tooling process. Furthermore, the viscosity of a polymer is also affected by the degree of cure of the polymer and it increases as the molecular weight of the reacting polymer increases. However, in the present application of soft tooling process, the problem of flowability of composite polymer is of concern only during the pouring of mold material into the mold box. Generally, the task of filling mold material in the box is carried out within the pot life of the polymer (i.e., before the formation of gel). Therefore, the effect of curing is not considered in the equivalent viscosity of particulate filled flexible mold material.

Viscosity of the material was measured with stress controlled rotational rheometer (TA Instruments AR G2). Measurements were done with 20.0-mm plate geometry at room temperature. Zero shear viscosity values were recorded from creep curve at shear rate varied between 0.1 and 0.001 for 1 h. The gap size was used between 1.8 mm and 6.5 mm depending on the amount of filler in the melt composite. The optimum gap size was estimated based on the study reported by Barnes.[61] For the measurements, the liquid polymer and the filler were mixed properly, hardener was added and the material was poured into the measuring plate instantaneously.

Experimental results and discussion

The used gap sizes and shear rates were optimized based on flow curve measured from 0.01 1/s to 10 1/s. At the lowest shear rate (0.01 1/s) the measurement is performed close to the limit of sensitivity. Therefore some scattering occurs. The flow curves as shown in Figure 8 are chosen as an example, because the parameters used in creep measurements of corresponding matrix-filler composite are the most representative regarding the whole set of measurements. In Figure 8, it can be seen that shear-

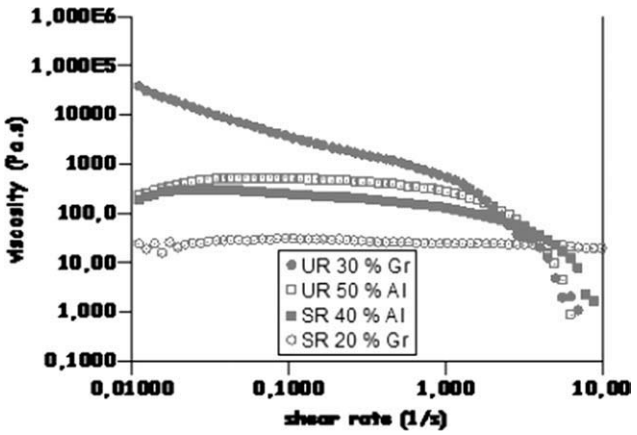

Figure 8 Flow curve of polyurethane and silicone rubber suspensions with aluminum and graphite filler.

thinning behavior of polyurethane fluid starts at the speed of shear rate around 1.0 1/s. The same kind of behavior was seen in all of the materials (data not shown), except those which do not exhibit yielding behavior (e.g., SR with 20% Gr). On the basis of the results, it is found that using shear rate up to 0.1 1/s does not break down the structure of the material. Thus, the shear rate 0.1 1/s or less may describe zero shear viscosity. Therefore the creep measurements were done at 0.01 1/s or 0.1 1/s shear rate. The value of shear rate, 0.1 s^{-1} was chosen for lower viscosity samples to minimize scattering, whereas 0.01 1/s shear rate was chosen for the samples of higher viscosity to minimize possible decrease in viscosity due to shear thinning. The values of gap sizes and shear rates used for various suspensions during equivalent viscosity measurements are reported in Table III. Table III also lists the average measured values of equivalent viscosities of more than one sample (three to four samples) of melt PU/SR filled with Al/graphite filler for different volume fraction of filler.

The viscosity measurements are performed at 23°C and all the viscosities reported in this study are the values at very low shear rates, in which the samples show Newtonian behavior. Since, the flexible mold materials are the kind of reactive thermosetting resin, where the viscosity increases by progression of the curing reactions (reaction conversion) and at a specified conversion, called gel conversion, the viscosity approaches infinity.

The experimental viscosity values with higher loading of particles are found to be extremely high. Practically, it was impossible to get uniformly mixed material at such a high packing levels. The particles were not fully attached to polymer molecules, and some air gaps were present between the matrix and the particles. Since the amount of polymer was not high enough to fill the gap between the particles in composite, there no viscose behavior in the material existed, which exhibit infinite viscosity value.

Equivalent viscosity model

Prediction of suspension viscosity has been the subject of many investigations for around a century, and the literature on particulate suspensions is truly immense. In the application of soft tooling processes, the concentration level of filler particles in the matrix is not strict to a fixed range; rather it varies from low concentrations to high concentrations to achieve the desired properties of mold materials. Practically, the filler particles available in the market are not uniform and belonged to a particular shape. The primary aim of this investigation is to find a suitable (generalized) model to make better prediction of equivalent viscosity for irregular particle filled flexible mold material for using in soft tooling processes through an extensive survey on different

TABLE III
Used Gap Sizes and Shear Strains in Viscosity Measurements

Sample	Filler (%)	Gap size (mm)	Strain (1/s)	Zero shear viscosity (Pas)
Polyurethane with aluminum	0	2.0	0.1	3.5195
	10	1.8	0.1	6.1498
	20	1.9	0.1	9.8171
	30	2.6	0.1	13.94
	35	2.2	0.1	44.911
	40	2.6	0.1	79.814
	45	3.4	0.1	245.26
	50	3.6	0.1	727.96
	60	6.5	0.01	23,687.0
Polyurethane with graphite	10	2.5	0.1	6.9168
	15	2.5	0.1	13.547
	20	2.5	0.1	35.761
	25	2.9	0.1	119.087
	30	4.0	0.1	398.11
	35	5.0	0.01	7327.4
	40	5.5	0.01	40,430.0
	45	6.5	0.001	301,000.0
Silicone with aluminum	0	2.0	0.1	5.2928
	10	2.0	0.1	6.7751
	20	2.0	0.1	12.247
	30	2.8	0.1	34.966
	35	2.8	0.1	74.159
	40	4.0	0.1	260.41
	45	4.0	0.01	2186.3
	50	4.0	0.01	13,340.2
	60	4.0	0.01	45,945.0
Silicone with graphite	10	1.5	0.1	11.468
	15	1.6	0.1	20.303
	20	2.0	0.1	48.394
	25	2.8	0.01	176.86
	27.5	2.8	0.01	433.42
	30	3.0	0.01	1539.1
	35	5.0	0.01	8477.1
	40	6.0	0.01	29,844.0

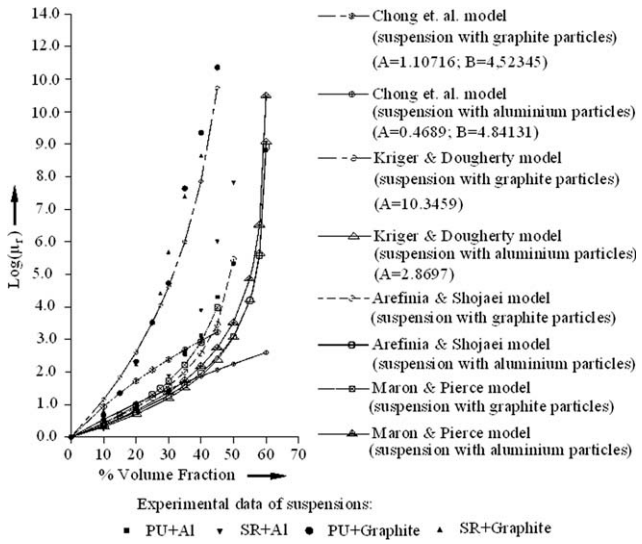

Figure 9 Comparison of various relative viscosity models with experimental data.

existing equivalent viscosity models reported in the literatures.

Figure 9 illustrates the experimental results of relative viscosities of suspensions (containing silicone rubber and polyurethane filled) with volume fractions of graphite and Al particles as well as the predictive results obtained by various models. In the Figure 9, the experimental values of relative viscosity of particle reinforced melt mold composites are shown as points, whereas the models are represented by the lines with different symbols indicating different models. The controllable parameters of each model in the present work are determined using a well-established population based global optimization technique, Genetic Algorithm (GA). In GA-based optimization method, the GA-parameters (namely population size, crossover probability, and mutation probability) are kept same to find the optimum values of controllable parameter(s) for all models to assure better comparisons. The percentage deviations of model estimations from the experimental results for both the suspension systems of flexible mold materials with Al and Graphite fillers are found as enlisted in Table IV. By comparing the experimental data of SR and PU suspensions with the results of various models, it is found that the generalized model of Arefinia and Shojaei[64] [defined in eq. (16), where the values of a and b are 0.3 and 2, respectively, and φ is the volume fraction of filler particle in the suspension] holds the supremacy among other models in case of suspension with Al. On the other hand, Kriger and Dougherty model [expressed in eq. (17)][63] shows better explanation to the experimental data over other models. Therefore, it is showed that the generalized model is not able to explain all the measured experimental data of suspension of particle-reinforced flexible mold materials, particularly when the filler particle size is quite large. From Figure 9, it is seen that for low concentration of filler (less than 10%), the generalized model fits well with the experimental data of both the Al and graphite filled suspensions. By using the experimental data of suspension with Al particles to estimate the values of controllable parameters (a and b) of eq. (12), interestingly, it has been found that using GA-based optimization method, the obtained values of a (=0.316) and b (=2.045) are very close to the values of controllable parameters of the generalized model of Arefinia and Shojaei, yielding to an average error 43.56%. However, though the performance of Arefinia and Shojaei model is seen quite well in both the SR and PU composites filled with Al particles, it is not so in the composites with graphite particles (showing an average percentage error 70.56) which are of larger sizes compared to Al particles. This suggests that the generalized model of Arefinia and Shojaei has some limitations in the extent of filler particle size. Basically, the controllable parameters (a and b) in Arefinia and Shojaei model[64] whose values are 0.3 and 2.0, are determined based on the experimental data of suspensions namely (hydroxyl terminated polybutadiene) HTPB/Al, HTPB/AP (ammonium perchlorate) and PBN/Al where the maximum value of (avg.) particles size was limited to 144 μm.

TABLE IV
Average Percentage Deviations of Model Estimation from Experimental Results for Various Models

		Average percentage deviation of estimations for suspensions of flexible mould material	
Sl. No.	Model	Graphite	Aluminum
1	Maron-Pierce's model[57]	69.916	80.338
2	Chong et al. model[58]	58.852	53.376
3	Krieger-Dougherty's model[59]	41.911	46.001
4	Arefinia-Shojaei's model[60]	70.560	43.988

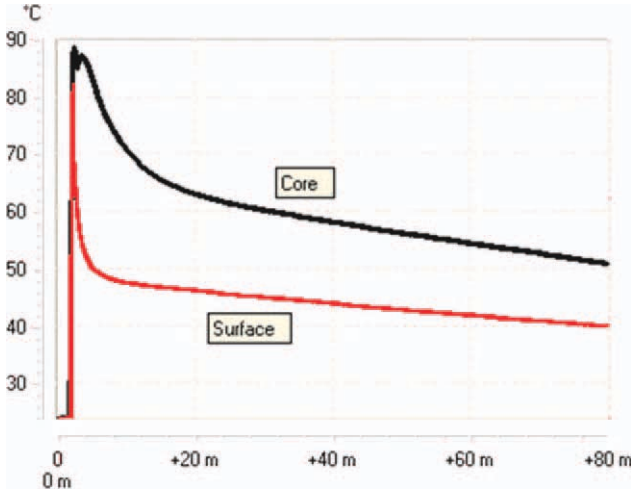

Figure 10 Cooling rate of wax pattern using PU mold of 30 mm wall thickness at room temperature. [Color figure can be viewed in the online issue, which is available at wileyonlinelibrary.com.]

$$\eta_r = \left(1 - \frac{\varphi}{\varphi_m}\right)^{a\left(\frac{\varphi}{\varphi_m}\right)-b}, \tag{16}$$

$$\eta_r = \left(1 - \frac{\varphi}{\varphi_m}\right)^{-A\varphi_m}. \tag{17}$$

EXPERIMENTATION OF COOLING TIME IN ST PROCESS

In this experimental study, PU is considered as the mold material, and Al particle is taken as filler material. The cooling time required is compared in the case of using Al-filled PU composite mold material with that of using only PU for producing a cubical shaped (size: 50 mm × 50 mm × 50 mm) wax component. The experimentation is carried out with the amounts of Al filler content in PU mold material is 23.8% of volume fraction. In this study, Investment casting wax (A7-11) supplied by Blayson Olefines Ltd, UK is used. The wax consists of natural wax, synthetic wax and natural resins. The melting point of wax is 55–70°C and the boiling point/flash point is greater than 200°C. The melt wax possesses viscosity of 0.6 Pas at around 100°C. A cubical shaped RP component made using StereoLithography Apparatus (SLA) is used as a pattern for making the mold. Two thermocouple wires are placed on the upper part of the mold box for measuring the temperatures. The cooling/solidification of liquid wax is carried out at room temperature.

Results and discussions

The behaviors of cooling rate of the cubical shaped wax component where the mold wall thickness is kept as 30 mm and the outside temperature of mold box is the ambient condition (25°C) are demonstrated here. The variations of temperature with time at the location of 5 mm deep from the surface and the core of wax component using PU mold material are plotted in Figure 10. In Figure 11, variations of temperature at the same positions of wax component using Al particle reinforced PU mold material are shown. In the experimental study of cooling time in Soft Tooling process, the temperature measurements were carried out through data acquisition system using thermocouple wires. The data acquisition system starts to take reading of temperature before pouring the molten wax into the mold cavity. For this reason, the first vertical line (from left) is seen in both the Figures 10–11. Moreover, during experimentation, measurement of temperature and pouring of molten wax into the mold cavity were carried out simultaneously. As a result, sometimes disturbances of recording of temperature through thermocouple may have occurred. Some of the vertical lines found in Figure 11 represent such disturbances of temperature measurement. In both the Figures 10 and 11, it is noticed that initially, cooling rate near to the surface of component is much faster than that at the core. This is because, heat near the surface of wax pattern dissipated only through the mold wall. Whereas heat at the core of wax pattern flows through the mold wall as well as (solidified) wax and the thermal conductivity of wax is quite lower than the mold material. After certain time, both the temperatures gradually come to the atmospheric one. The temperature of liquid wax during pouring in both the molds made of PU and Al particle reinforced PU is kept almost same as 85°C. Figure 10 demonstrates that to reach the temperature, for instance 40°C at a depth of 5 mm from the surface of wax component, it takes around 80 min in case of PU mold, where as only 25 min is

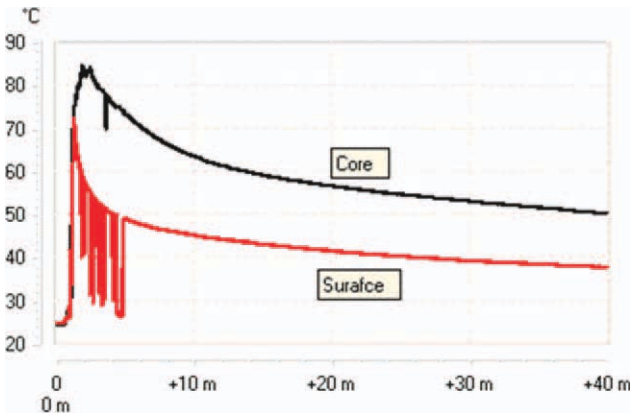

Figure 11 Cooling rate of wax pattern using Al particle reinforced PU mold of 30 mm wall thickness at room temperature. [Color figure can be viewed in the online issue, which is available at wileyonlinelibrary.com.]

required in case of particle reinforced PU. Thus, it is revealed that the cooling time is reduced significantly in soft tooling process using particle-reinforcement with mold materials. This happens due to the increase of effective thermal conductivity of mold material. However, besides the thermal conductivity of mold material, the cooling time also depends on the temperature difference between the inside and outside of mold box, and thickness of mold wall.

DIFFERENT ASPECTS IN REDUCING COOLING TIME IN ST PROCESS AND FURTHER ACTIVITIES ON THIS RESEARCH WORK

The process (as illustrated in Fig. 1) involves making of the master pattern (namely Rapid Prototype model) using any rapid prototyping techniques (say, StereoLithography Apparatus, SLA). This pattern is finished to a desired quality which is used in ST process. As discussed earlier, the mold material should be highly thermally conductive to reduce the cooling time. But, as the thermal conductivities of conventional flexible (polymeric) mold materials are very low, the approach of inclusion of thermally conductive fillers into mold material increases the cooling rate by increasing effective thermal conductivity of mold material. However, from the above experimental studies it is observed that though inclusion of fillers into mold material enhances the effective thermal conductivity of the mold as a result the cooling time in soft tooling process is reduced it also increased the effective modulus of elasticity as well as the equivalent viscosity of the molten mold material. The stiffness of mold box becomes high with increasing the modulus of elasticity of mold material, which also depends on the size and shape of the wax component to be manufactured. High stiffness of mold box creates many difficulties namely removing the pattern from the mold box. Therefore, the modulus of elasticity of mold material should not be higher than a limiting value corresponding to the wax component. Even though, as low as possible the value of modulus of elasticity will be better in ST process. On the other hand, increase of effective viscosity reduces the flow-ability of the melt mold material. In ST process, pouring of melt (polymeric) mold material into mold box should be carried in such a way that the mold material fills up the entire mold box cavity before the formation of gel, i.e., within the pot life of the polymer. Low viscosity value of the melt polymer can fulfill this objective easily. Therefore, the viscosity of the mold material should be near to the limiting value. Here also, the limiting value of effective viscosity depends on the size and shape of the wax component to be manufactured.

In the above experimental studies, it suggests that the amount of filler content (volume fraction), size, and shape factor of filler particle play important roles in the effective thermal conductivity and modulus of elasticity of particle reinforced flexible mold materials. Furthermore, the equivalent viscosity of (melt) particle reinforced flexible mold materials depends on the volume fraction of filler particle as well as the maximum packing fraction of reinforced particles which is also related to the size and shape distributions of filler particles. Therefore, to achieve best results (i.e., lowest time requirement in solidification of wax/plastic with obtaining other processing advantages) in ST tooling process, the effective thermal conductivity of mold material should be high enough, associated with the effective modulus of elasticity. Further equivalent viscosity of mold material should have the acceptable values for a given configuration of wax/plastic pattern. In other way, effective thermal conductivity should be a maximum value while the values of modulus of elasticity and viscosity should be as low as possible. It can be achieved by finding the optimized values of the controlling parameters, namely volume fraction, size and shape factor of filler particle for a given particle reinforced flexible mold material composite system. In case of a given size and shape distributions of filler particles, the only controlling parameter, volume fraction of filler needs to be optimized. Since, in this optimization process there are three primary objectives (maximization of thermal conductivity, minimization of modulus of elasticity and minimization of viscosity) and these objectives are contradictory with each others, it can be solved by suitable multi-objective optimization tool. The authors are presently working on this issue.

CONCLUDING REMARKS

To reduce the cooling time in ST process, the effective thermal conductivity of mold material is increased by introducing conductive filler particles into mold material. Since the presence of conductive filler affects other mold properties, in this work the equivalent thermal properties, equivalent modulus of elasticity and equivalent viscosity of particle reinforced flexible mold materials (PU and SR) with Al and graphite powder are experimentally analyzed. The experimental results of these properties of particle reinforced flexible mold materials are explained with the related existing models reported in literature. It has been found that with increase in the effective thermal conductivity, the equivalent modulus of elasticity and viscosity are also increasing, those are primarily dependent upon the parameters namely type of flexible mold material, type of filler material, the amount of filler content in the

composite and the size and shape distributions of the filler particles. To obtain best results in ST tooling process (i.e., lowest time requirement in solidification of wax/plastic with obtaining other processing advantages), it is proposed that the above controlling parameters are to be optimized using suitable multi-objective optimization tool based on the models of equivalent thermal conductivity, modulus of elasticity and viscosity of particle reinforced flexible mold material.

The authors would like to thank the reviewers for their valuable and helpful comments that lead to a significant improvement of the article.

References

1. Rosochowski, A.; Matuszak, A. J Mater Process Technol 2000, 106, 191.
2. Agrawal, R.; Saxena, N. S.; Mathew, G.; Thomas, S.; Sharma, K. B. J Appl Polym Sci 2000, 76, 1799.
3. Boudenne, A.; Ibos, L.; Fois, M.; Gehin, E.; Majeste, J. C. J Polym Sci Part B: Polym Phys 2004, 42, 722.
4. Iqbal, A.; Frormann, L.; Saleem, A.; Ishaq, M. Polym Compos 2007, 28, 186.
5. Keith, J. M.; King, J. A.; Lenhart, K. M.; Zimny, B. J Appl Polym Sci 2007, 105, 3309.
6. Miller, M. G.; Keith, J. M.; King, J. A.; Edwards, B. J.; Klinkenberg, N.; Schiraldi, D. A. Polym Compos 2006, 27, 388.
7. Mu, Q.; Feng, S.; Diao, G. Polym Compos 2007, 28, 125.
8. Ng, H. Y.; Lu, X.; Lau, S. K. Polym Compos 2005, 26, 778.
9. Oliveira, F. A.; Alves, N.; Giacometti, J. A.; Constantino, C. J. L.; Mattoso, L. H. C.; Balan AMOA, Job, A. E. J Appl Polym Sci 2007, 106, 1001.
10. Razzaq, M. Y.; Frormann, L. Polym Compos 2007, 28, 287.
11. Subodh, G.; Manjusha, M. V.; Philip, J.; Sebastian, M. T. J Appl Polym Sci 2008, 108, 1716.
12. Tsukuda, R.; Sumimoto, S.; Ozawa, T. J Appl Polym Sci 1997, 63, 1279.
13. Vinod, V. S.; Varghese, S.; Kuriakose, B. J Appl Polym Sci 2004, 91, 3156.
14. Wang, L.; Li, F.; Su, Z. J Appl Polym Sci 2008, 108, 2968.
15. Wang, Q.; Gao, J.; Wang, R.; Hua, Z. Polym Compos 2001, 22, 97.
16. Wong, C. P.; Bollampally, R. S. J Appl Polym Sci 1999, 74, 3396.
17. Yu, S.; Hing, P.; Hu, X. Compos A: Appl Sci Manufact 2002, 33, 289.
18. Xu, Y.; Chung, D. D. L.; Mroz, C. Compos A: Appl Sci Manufact 2001, 32, 1749.
19. Weidenfeller, B.; Hofer, M.; Schilling, F. R. Compos A: Appl Sci Manufact 2004, 35, 423.
20. Sundstrom, D. W.; Chen, S. Y. J Compos Mater 1970, 4, 113.
21. Mamunya, Y. P.; Davydenko, V. V.; Pissis, P.; Lebedev, E. V. Eur Polym J 2002, 38, 1887.
22. Lopes, C. M. A.; Felisberti, M. I. Polym Test 2004, 23, 637.
23. Kim, S. W.; Choi, B.; Lee, S. H.; Kang, K. H. High Temperatures-High Pressures 2008, 37, 21.
24. Ishida, H.; Rimdusit, S. Thermochimica Acta 1998, 320, 177.
25. Ye, C. M.; Shentu, B. Q.; Weng, Z. X. J Appl Polym Sci 2006, 101, 3806.
26. Yung, K. C.; Liem, H. J Appl Polym Sci 2007, 106, 3587.
27. Lee, G. W.; Park, M.; Kim, J.; Lee, J. I.; Yoon, H. G. Compos A: Appl Sci Manufact 2006, 37, 727.
28. Tavman, I. H. Powder Technol 1997, 91, 63.
29. Rusu, M.; Sofian, N.; Rusu, D. Polym Test 2001, 20, 409.
30. Mayadunne, A.; Bhattacharya, S. N.; Kosior, E. Plast Rubber Compos Process Appl 1996, 25, 126.
31. Mooney, M. J Colloid Sci 1951, 6, 162.
32. Gustafsson, S. E. Rev Scientific Instruments 1991, 62, 797.
33. Gustavsson, M.; Karawacki, E.; Gustafsson, S. E. Rev Sci Instrum 1994, 65, 3856.
34. Log, T.; Gustafsson, S. E. Fire Mater 1995, 19, 43.
35. Bohac, V.; Gustavsson, M. K.; Kubicar, L.; Gustafsson, S. E. Rev Sci Instrum 2000, 71, 2452.
36. He, Y. Termochimica Acta 2005, 436, 122.
37. Agari, Y.; Uno, T. J Appl Polym Sci 1985, 30, 2225.
38. Agari, Y.; Uno, T. J Appl Polym Sci 1986, 32, 5705.
39. Maxwell, J. C. A. A Treatise on Electricity and Magnetism, 3rd ed.; Dover: New York, NY, 1954; Chapter 9.
40. Cheng, S. C.; Vachon, R. I. Int J Heat Mass Transfer 1969, 12, 249.
41. Butta, E.; Migliaresi, C. Materiali compositi a matrice polimerica, AIMAT Manuale dei Materiali per l'Ingegneria. Mc. Graw Hill, 1996, ISBN-883863211-1.
42. Bruggeman, D. A. G. Berechnung Verschiedener physikalischer konstanten von heterogenen substanzen. Ann Phys (Leipzig) 1935, 24, 636.
43. Lewis, T. B.; Nielsen, L. E. J Appl Polym Sci 1970, 14, 1449.
44. Torquato, S. J Appl Phys 1985, 58, 3790.
45. Gere, T. M.; Timoshenko, S. P. Mechanics of Materials; Brooks Cole: Monterey, CA, 1984.
46. Moore, P. Am Soc Nondestructive Test 2007, 7, 319.
47. Paul, B. Trans Metall Soc AIME 1960, 218, 36.
48. Ravichandran, K. S. J Am Ceram Soc 1994, 77, 1178.
49. Wu, T. T. J Appl Mech 1965, 32, 211.
50. Hashin, Z.; Shtrikman, S. J Mech Phys Solids 1963, 11, 127.
51. Halpin, J. C. J Compos Mater 1969, 3, 732.
52. Halpin, J. C.; Kardos, J. L. Polym Eng Sci 1976, 16, 344.
53. Walpole, L. J. J Mech Phys Solids 1966, 14, 151.
54. Walpole, L. J. J Mech Phys Solids 1966, 14, 289.
55. Voigt, W. Ann Phys 1889, 38, 573.
56. Reuss, A.; Berechnung der Fliebgrenze von Mischkristallen auf grund der Plastizitatsbedingung fur Einkristalle, ZAMM 1929, 9, 49.
57. Benveniste, Y. Mech Mater 1987, 6, 147.
58. Kroner, E. Zeitschrift für Physik 1958, 151, 504.
59. McLaughlin, R. Int J Eng Sci 1977, 15, 237.
60. Lielens, G.; Pirotte, P.; Couniot, A.; Dupret, F.; Keunings, R. Compos A: Appl Sci Manufact 1998, 29, 63.
61. Barnes, H. A. J Non-Newtonian Fluid Mech 2000, 94, 213.
62. Maron, S. H.; Pierce, P. E. J Colloid Sci 1959, 11, 80.
63. Chong, J. S.; Christiansen, E. B.; Baer, A. D. J Appl Polym Sci 1971, 15, 2007.
64. Krieger, I. M.; Dougherty, T. J. J Rheol 1959, 3, 137.
65. Arefinia, R.; Shojaei, A. J Colloid Interface Sci 2006, 299, 962.